



# Application Flatness Technique for Intelligent Control of a New Electric Energy Source

Mohsen Radan

Electrical Power Engineering Group, Najafabad Branch, Islamic Azad University, mohsenradan69@gmail.com

---

## Abstract

In this paper, an intelligent control strategy based on combination of the “flatness based control technique” and the “perturbation and observation (P&O) MPPT algorithm” is developed and investigated to control a hybrid electric energy source (HEPS). This EHPS is composed of a fuel cell system (FC) and a solar panel (SP), as the main source and a super capacitor bank (SC), as the auxiliary sources. The main property of this strategy is that the system power flow is managed in different operating modes with the same control algorithm (without algorithm commutation). The power flows between the fuel cell, the SC is controlled by the flatness based control technique while a P&O MPPT technique is developed to control power of the SP. To validate performance of the proposed control of the HEPS, the simulation results are presented.

*Keywords:* Flatness, Hybrid energy source, Full cell, MPPT.

*Article history:* Received 12-December-2017; Revised 04-January-2017; Accepted 13-February-2017.

© 2016 IAUCTB-IJSEE Science. All rights reserved

---

## 1. Introduction

Rapid increasing of the population and energy consumption in the world, increasing global warming and greenhouse gas emissions are justifiable reasons for using the clean and renewable energy instead of fossil-fuel [1]. Between the renewable energy sources, photovoltaic systems have increasing roles in modern electric power technologies, providing secure and pollution-free power sources. Solar arrays are the primary source of photovoltaic systems. They are dependent energy sources with nonlinear  $V-I$  characteristics under different environmental (insolation, temperature and degradation) condition, high fabrication cost and low energy conversion efficiency [2]. Another energy source which has been attracted attention of the researchers in various applications is fuel cell (FC). To compensate the well-known weakness of FCs like low dynamics of some fuel cells (especially during start-up and transient state of load demands), and to absorb the braking energy, they are usually utilized in association with one or more energy storage devices like the bank of super capacitors (SCs) or the bank of batteries (BAT) [3-4]. In this paper, a bank of SCs is used in the hybrid

system as it has some advantages such as: huge capacitance, weak series resistance and high specific energy [5-6] in comparison with the BATs. Because of these reasons super capacitors has been used in various field such as voltage regulation of industrial network [7], electrical vehicle [8]. To control the power flow between the energy sources, energy storage devices and the electrical load, the different type of hybrid electric systems and different control methods have been proposed. In [9], the authors propose a method with different algorithms such that in each operating mode, one of control algorithms is applied. Hence, the algorithm commutation is necessary when the operating mode changes which may lead to a “chattering” phenomenon. In [10-11], a flatness based method is used to control a FC/SC hybrid system without the algorithm commutation. This method is useful when explicit trajectories are required. The flatness based control technique has some advantages: the system behavior can be predicted with this technique even during the transient state. Furthermore, dynamics of the system which is controlled with this method is high [10-11].

In the present paper, an intelligent control method is presented to manage the power flow in a hybrid electric source composed of the energy sources, a fuel cell and a solar panel, and an energy storage device, a SC. Fig. 1 shows the topology of the studied hybrid system. The control strategy is based on a combination of the flatness based control technique to manage the energy between FC and SC, and a P&O MPPT algorithm to control the SP power. In the following, the system will be described and the mathematical model will be presented. Then, the control strategy will be explained and finally, the simulation results will be presented to validate the proposed control strategy.

**2. System Description**

Fig. 1 shows the model of the hybrid electric energy source. This system is composed of:

- A fuel cell connected to a low voltage DC-bus v1,
- A SC as the auxiliary source (storage device), connected to the low voltage DC-bus via a bidirectional DC-DC converter1. The low-voltage DC-bus has a variable voltage to control the dynamics of the fuel cell and to manage the energy flow between FC and SC.
- A high voltage DC-bus v2 to keep the load voltage into a constant desired value. The high voltage DC-bus is connected to the low voltage one through the bidirectional DC-DC converter2.
- A SP which is connected to the high voltage DC-bus via a boost DC-DC converter3.
- A variable load which is modelled by a variable current source.

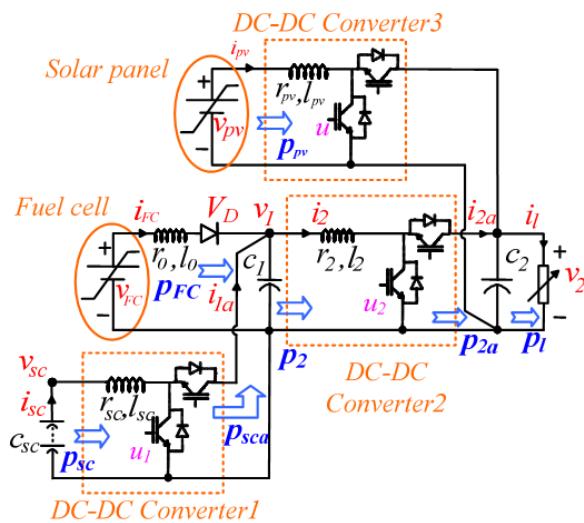


Fig. 1. Electrical model of the hybrid power source.

In this study, the cable inductance, the converters power losses and the serial resistances of the capacitors are neglected.

**3. Mathematical Model**

*A) Fuel cell*

The voltage/current characteristic of fuel cell is a nonlinear characteristic which can be expressed by [12]:

$$V_{fc} = E - A \ln\left(\frac{i_{fc} + i_o}{i_o}\right) - R_m(i_{fc} + i_n) + B \ln\left(1 - \frac{i_{fc} + i_n}{i_L}\right) \quad (1)$$

Where  $E$  is the open circuit voltage of the fuel cell,  $i_{FC}$ ,  $i_o$  and  $i_L$  show the delivered current, the exchange current and the limiting current, respectively. Also,  $A$  and  $B$  stand for slopes of the Tafel line and the constant in the mass transfer.  $I_n$  represents the internal current and finally,  $R_m$  is the membrane and contact resistances. Fig. 3 shows v-i static characteristic of a typical FC according to equation (1) which is used in the HEPS as one of the energy sources.

*B) Solar cell*

Like FCs, solar cells have nonlinear voltage/current characteristics. These v-i characteristics depend on insolation and temperature and so, their operating point depends on the environmental and load conditions. Using the equivalent circuit of solar cells presented on Fig.4, the nonlinear v-i characteristic of a solar panel with  $M$  parallel strings and  $N$  series cells per string is [12].

$$V_{pv} = \frac{N}{\lambda} \ln\left(\frac{I_{PH} - i_{pv} + I_o}{MI_o}\right) - \frac{N}{M} R_s i_{pv} \quad (2)$$

where  $v_{pv}$  and  $i_{pv}$  are the output voltage and current of the solar panel, respectively,  $I_{PH}$  is the generated current under a given insolation condition,  $I_o$  is the reverse saturation current,  $R_s$  stands for the series resistance of the solar cell and  $\lambda$  is a constant coefficient that depends on cell material and temperature. Fig. 4 shows the I-V static characteristic of a typical solar panel according to the equation (2) for different values of temperature ( $15^\circ C < T < 55^\circ$ ) and insolation ( $400W/m^2 < G < 1200W/m^2$ ). This equation is used to model the solar panel in the HEPS.

**4. Flatness Based Control**

In this section, we present the one-loop flatness-based controller. The FBC strategy has been chosen because of its use fullness in situations where explicit trajectory generation is required [10], [11]. In fact, the behavior of the system state variables can be planned owing to given reference trajectories. The control structure consists of an

electrostatic energy loop which allow flat three-phase voltage network with the desired magnitude and frequency and those with a low harmonic distortion rate. The concept of flat systems was introduced by Fliess et al.[12] using the formalism of differential algebra. In differential algebra, a system is considered to be differentially flat if a set of variables (flat output components) can be found such that all state variable and input components can be determined from these output components without any integration [13]. The state and input variables can be directly expressed, without integrating any differential equation, in terms of the flat output and a finite number of its derivatives. Moreover, in our particular application, the number of sensors is reduced. The implementation of the control law does not use inductive current measurements. Only load current sensors are used for generating the control law. Another interesting point to underline is that the use of reference trajectories of the flat outputs allows ensuring safe operation during the start-up. The fact that the flat controllers use the reference reactions instead of disturbance reactions reduces the noise impact. Indeed, the derivative terms in control laws are less affected by noise. For the control of differentially flat systems, one concentrates on generating feasible trajectories rather than trying to force the system trajectory to converge toward given operating point. With the flat approach, transient state can be analytically fore seen which is not the case with classical approaches. Contrary to classical approaches where the dq output volt-ages are controlled, we propose to control the dq electrostatic stored in the output capacitances. In fact, this choice should lead to a better dynamical behavior as regards load perturbations when the three-phase inverter supplies constant power load systems. Thus we propose to assume that the electrostatic energy is the candidate flat output the unstable dynamic zeroes which cannot be guaranteed for other types of dynamical systems. Equations (12-17) explaining Flatness Technique quite [10, 12, 13].

$$\begin{cases} \dot{x}(t) = f(x(t), u(t)) \\ y(t) = h(x(t), u(t)) \end{cases} \quad (3)$$

$$u = [u_1, u_2, \dots, u_m]^T \quad (4)$$

$$x = [x_1, x_2, \dots, x_n]^T, \quad n \geq m \quad (5)$$

$$y = \phi[x, u, \dot{u}, \dots, u^{(\alpha)}], \quad \text{rank}\{\phi\} = m \quad (6)$$

$$x = \varphi[y, \dot{y}, \dots, y^{(\beta)}], \quad \text{rank}\{\varphi\} = n$$

$$u = \psi[y, \dot{y}, \dots, y^{(\beta+1)}], \quad \text{rank}\{\psi\} = m \quad (7)$$

The unique feature of allowing a parameterization of all system variables makes of flatness a tool for analysis revealing the nature of each system variable in its isolated relation with a centrally important set of variables from view point of controllability and observability. The invertible parameterization, involved in the flat outputs definition, thus creates a local bijection between system state solutions and arbitrary trajectories in the flat output space. There is no uniqueness of the flat output even if there is usually a favorite flat output expressing physical properties. The concept of flatness scan be seen as a nonlinear generalization of the Kalman's controllability and of the Brunovsky decomposition. Hence every linear controllable system is flat. More recently, flatness has been defined in a more geometric context, where tools for nonlinear control are more commonly available. There are two different geometric frameworks for studying flatness and provide constructive methods for deciding the flatness of certain classes of nonlinear systems and for finding these flat outputs if they exist. One approach is to use exterior differential systems and regard a nonlinear control system as an affine system on an appropriate space [12]. In this context, flatness can be described in terms of the notion of absolute equivalence defined by Cartan [13]. Another geometric approach to study flatness is by using "JetBundles". In this paper a somewhat different geometric point to view is adopted, relying on a Lie-Backlund framework as the underlying mathematical structure. It offers a compact framework in which to describe basic results and is also closely related to the basic techniques that are used to compute the functions that are required to characterize the solutions of flat systems (the so-called flat outputs). In jet bundle approach a mapping from an infinite dimensional manifold whose coordinates are not only made up of original variables but also of jets of infinite order is dealt. Figure.2 shows special concept of flatness [11,13,14].

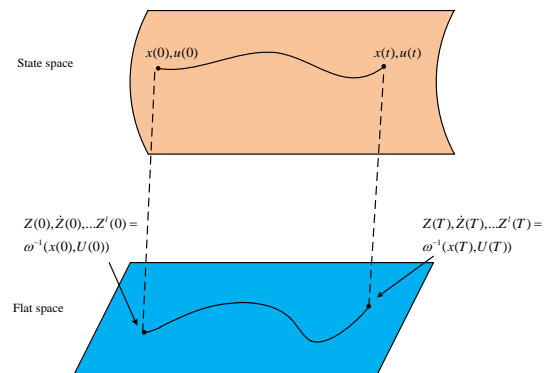


Fig. 2. Espetial concept of flatness

A) Interest of the Flatness-Based Approach

Some properties of the flat systems are suitable for their control. From [14], we can list the main advantages for power applications. The fact that the flat controllers use the reference reactions instead of disturbance reactions reduces the noise impact. Indeed, the derivative terms in control laws are less affected by noise. For the control of differentially flat systems, one concentrate on generating feasible trajectories rather than trying to force the system trajectory to converge toward a given operating point. With the flat approach, transient states can be analytically foreseen which is not the case with classical approaches. For flat systems, the application of the I/O exact feedback linearization technique does not lead to the occurrence of the unstable dynamic zeroes which cannot be guaranteed for other types of dynamical systems. Another interesting point to underline is that the use of reference trajectories of the flat outputs allows ensuring a safe operation during the start-up (see experimental part). Moreover, in our particular application, the number of sensors is reduced. The implementation of the control law does not use inductive current measurements. Only load current sensors are used for generating the control law

B) Flatness Property of the System

To develop the intelligent control strategy of the system, the flatness property should be study in the system. A system is flat if its state and control variable vector components are functions of flat output components [15]. To study the flatness in the system, the electrostatic energies stored in the DC bus capacitors, shown by  $y_1$  and  $y_2$ , are considered as the flat output components while the DC bus voltages  $v_1$  and  $v_2$  are the state variable vector components. It should be noted that in this study, the SC-bank voltage is considered as a variable parameter since its capacitance value is very high and its voltage variation by time is slow. Furthermore, the dynamics of the current loops are supposed to be widely faster than the voltage loop ones and so, currents  $i_{sc}$  and  $i_2$  (Fig. 1) are considered to follow perfectly their respective references. Therefore, the system order is reduced to two (with DC bus voltages  $v_1$  and  $v_2$  as state variable of the system).

The powers  $p_{sc}$  and  $p_2$  depicted in Fig.1, are control variables of the system. Such a system can be shown to be a flat system. The electrostatic energies  $y_1$  and  $y_2$ , components of the flat output vector are equal to:

$$y_1 = \frac{1}{2} c_1 v_1^2 \tag{8}$$

$$y_2 = \frac{1}{2} c_2 v_2^2 \tag{9}$$

Therefore, components of the system state variable vector are obtained as:

$$v_1 = \sqrt{\frac{2y_1}{c_1}} = \phi_1(y_1) \tag{10}$$

$$v_2 = \sqrt{\frac{2y_2}{c_2}} = \phi_2(y_2) \tag{11}$$

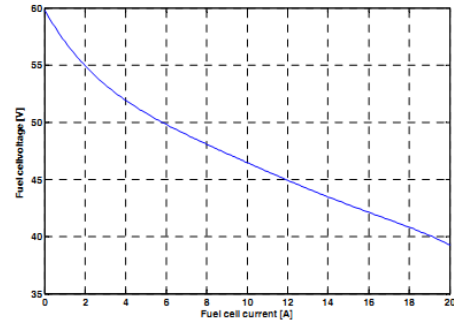


Fig. 3. Caractristic static of a typical fuel cell

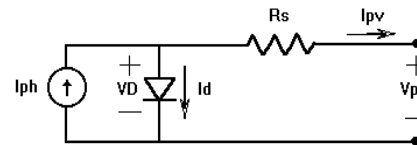


Fig. 4. Equivalent circuit of solar cells

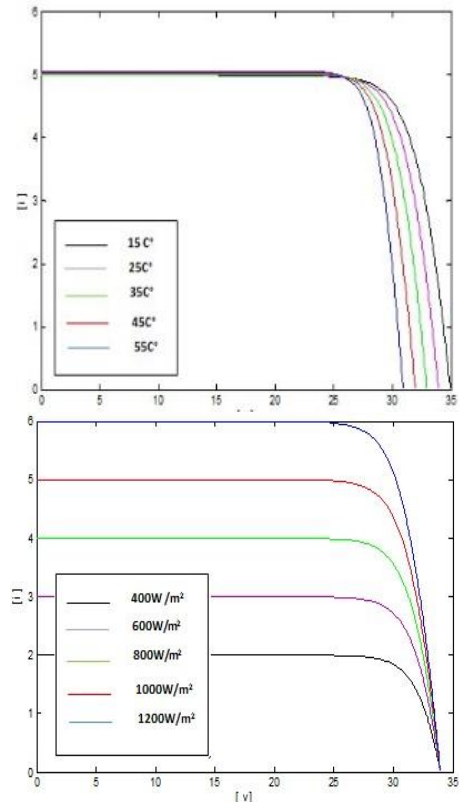


Fig. 5. I-V characteristic of a solar panel for different values of temperature(left Fig.) and insolation (right Fig.).

Components of the control variable vector of the system can be also calculated as follows:

$$p_2 = \frac{v_1^2}{2r_2} \left[ 1 - \sqrt{1 - \frac{4r_2(\dot{y}_2 + (p_l - p_v))}{v_1^2}} \right] = \phi_3(y_1, y_2, \dot{y}_2) \quad (12)$$

$$p_{sc} = \dot{y}_1 + (p_l - p_v) - p_{FC} - r_2 \left( \frac{p_2}{v_1} \right)^2 = \phi_4(y_1, \dot{y}_1, y_2, \dot{y}_2) \quad (13)$$

Therefore, the state and control variable vector components of the system are functions of flat output components  $y_1$  and  $y_2$ . Consequently, the studied system is a flat system. In the next section, the intelligent control strategy will be explained.

### 5. Control Strategy and Design of Reference Trajectories

To develop the control strategy, the system is divided by two subsystems: solar panel-load and fuel cell super capacitor bank. More precisely, the solar panel power is considered as a part of the load power. That means the SP can be controlled by a simple well-known control method, nonlinear control method, Maximum Power Point Tracking (MPPT) control strategy. This last one (MPPT algorithms) is used to improve the efficiency of the solar cells. The various MPPT algorithms are discussed in [14]. In this paper, the perturbation and observation (P&O) MPPT algorithm is employed to extract the maximum power from the SP. It measures the voltage, current, and power of the PV module and then perturbs the voltage to encounter the change direction. Fig. 6 shows the curve of the PV module. As shown in the left-hand-side MPP, the power of the PV is increased with increasing the voltage of the PV module until the MPP is reached. In the right-hand-side of the MPP, with increasing the voltage the power is decreased. That means if there is an increase in the power, the subsequent perturbation should be kept in the same direction until MPP is reached [15]. Fig. 7 shows the flowchart of P&O MPPT algorithm where Dis duty cycle of the DC-DC converter. To manage the energy in the second subsystem, the desired trajectories should be planned on the output variables of the system as the flat output prescribes directly the trajectories of all system variables. To control the system, the reference trajectories for  $y_2$  and  $y_1$  are designed as follows:

$$y_{2ref} = \frac{1}{2} \cdot c_2 \cdot v_{2ref}^2 \quad (14)$$

Since the output voltage should be a constant value ( $V_{2ref}$ ).

To calculate the  $y_{1ref}$ , the energy reference of the low voltage DC bus should be designed. For this purpose, a low pass filter is put into the

reference of  $y_1$  to limit dynamics of the power (or the current) delivered by the fuel cell [15]. Furthermore, the variable  $y_1$  has to be bounded to limit the power delivered by the power source (fuel cell). Consequently, the voltage across the capacitor  $c_1$  should belong to the interval  $[V_{FCmin}=f(i_{FCmax}), V_{FCmax}=f(0)]$ , where  $i_{FCmax}$  is the rated current of the fuel cell and  $f(i)$  stands for the function of V-I output characteristic of the fuel cell.

In steady state (normal mode), the power delivered by the fuel cell has to be equal to the load power; and the energy storage sources (SC) should be charged to its nominal value (i.e.  $v_{SC}=V_{SCref}$ ). If SC is so discharged, the voltage of FC should be decreased to deliver more energy toward SC and vice versa. For this purpose, the reference of  $y_1$  is calculated with respect to the SC voltage error:  $e_{SC} = V_{SCref} - v_{SC}$ . Fig. 7 shows block-diagram of the planned trajectory on  $y_1$ . To calculate the control variables of the system ( $p_2$  and  $p_{sc}$ ), the classical controllers are employed to ensure the energy references ( $y_{1ref}$  and  $y_{2ref}$ ) tracking:

$$y_i = \dot{y}_{iref} + k(y_{iref} - y_i) + k'(y_{iref} - y_i) \quad (15)$$

Where  $i=1,2$ . Substituting these values in equation (13-14) and dividing the calculated power to the concerned voltages, the current reference of the converters is calculated:

$$i_{2ref} = \frac{p_2}{v_1} \quad (16)$$

$$i_{scref} = \frac{p_{sc}}{v_{sc}} \quad (17)$$

Finally, the well-known hysteresis current regulators are employed to ensure the control of the current  $i_{SC}$  and  $i_2$  to their references  $i_{SCref}$  and  $i_{2ref}$  and generate the switch signals of the DC-DC converters 1 and 2.

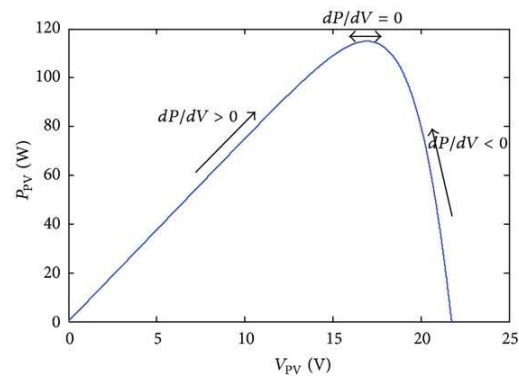


Fig. 6. Equivalent circuit of solar cells



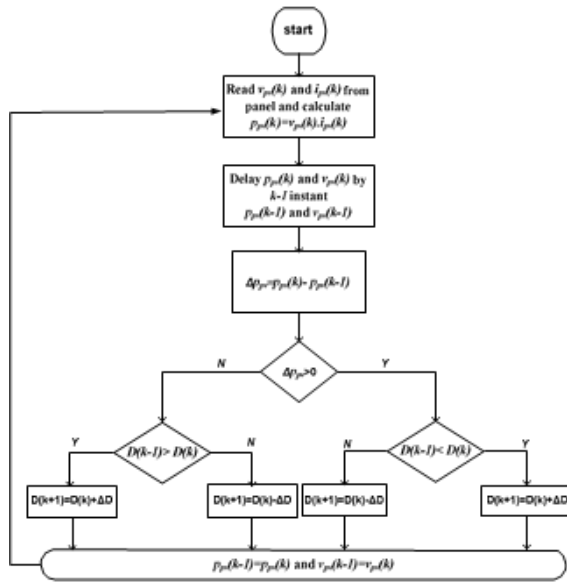


Fig. 7. Flowchart of P&O MPPT algorithm.

**6. Preference Validation**

The proposed control strategy is evaluated by extensive simulation of the hybrid system shown in Fig. 1 with the parameters listed in Table 1. Fig.9 shows current waveforms of the system in different operating mode. It consists of four parts: the FC and load currents,  $i_{FC}$  and  $i_l$ , are depicted in part (a), while the super capacitor current  $i_{sc}$  and its reference  $i_{scref}$  are presented in part (b). Current of the DC-DC converter2 is shown in the part (c) which follows its reference  $i_{2ref}$ . The SP current,  $i_{pv}$ , is presented in the part (d) which is a constant value equal to 5A. This value corresponds to the maximum power which can be extracted from the SP at standard temperature ( $T=25^\circ C$ ) and insolation  $G=1000W/m^2$ . It should be mentioned that negative load current is concerned to recovery operating mode which leads to charge the SC.

Fig.10 shows the voltage waveforms where the part (a) presents super capacitor voltage,  $v_{sc}$  and its reference value ( $V_{scref} = 24V$ ). The output DC-voltage,  $v_2$ , is depicted in part (b) which follows well its reference value, 100V. The voltage across the capacitor  $c_1$ ,  $v_{c1}$  is also presented in the part (c) of the Fig.9. As it is shown, this voltage is variable to control the power flow of the FC. It is controlled by the reference trajectory planned on  $y_1$ .

Fig. 11 shows the flat outputs,  $y_1$  and  $y_2$ , which track perfectly their references. The stored energy in the output capacitors,  $c_2$ , stays constant even if power load variation is intensive. On the other hand, to control dynamic of the FC and to manage energy in the systems, the stored electrostatic energy in DC-bus capacitors,  $c_1$ , is forced to vary slowly. When  $y_1$  reaches to its

minimum value, fuel cell delivers its maximum power to the system.

The powers of main source, ( $p_{FC}$ ), auxiliary source, ( $p_{sc}$ ), the input power of converter2, ( $p_2$ ), and the load and SP power are presented in Fig. 12. At the beginning,  $p_{sc}$  is negative which means the SC is charging as its voltage initial value is set to 23.7V.

Table.1.  
System Parameters

$V_{FCmax} = 60V$	$V_{FCmin} = 45V$
$V_{1ref} = 24V$	$V_{SP,OC} = 33.9V$
$V_{1ref} = 100V$	$P_{FCmax} = 500W$
$P_{SPmax} = 135W$	$c_1 = 330mF$
$c_1 = 13.6mF$	$c_{sc} = 290F$
$L_{sc} = 50\mu H$	$L_{pv} = 2.2mH$
$L_1 = 80\mu H$	$r_1 = 0.4$
$r_{sc} = 0.5m$	$r_f = 0.02$

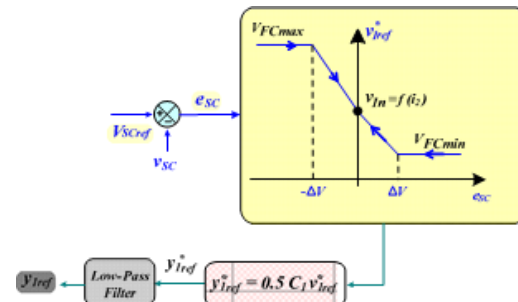


Fig. 8. Block diagram of  $y_1ref$  generation.

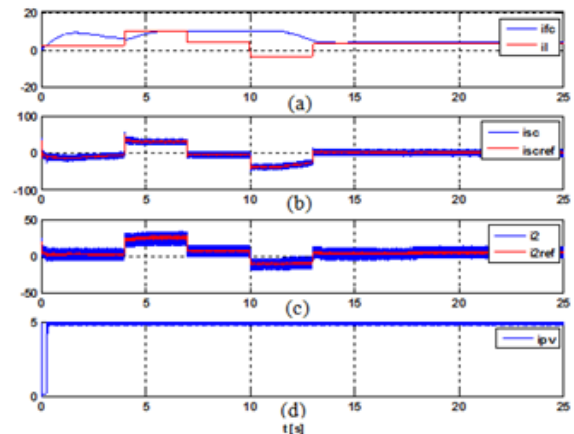


Fig. 9. Current waveforms of the system: (a) FC and load current;(b) supercapacitor current and its reference waveform;(c) current of the converter2 and its reference waveform; (d) SP current.

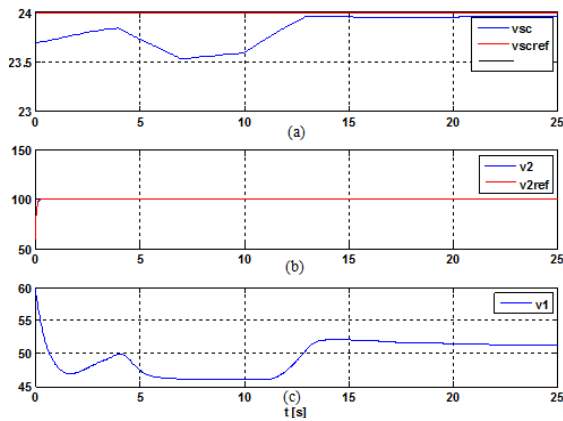


Fig. 10. Voltage waveforms of the system.(a) voltages across the super capacitor bank and its reference; (b) output voltage and its reference;(c) variable DC bus voltage.

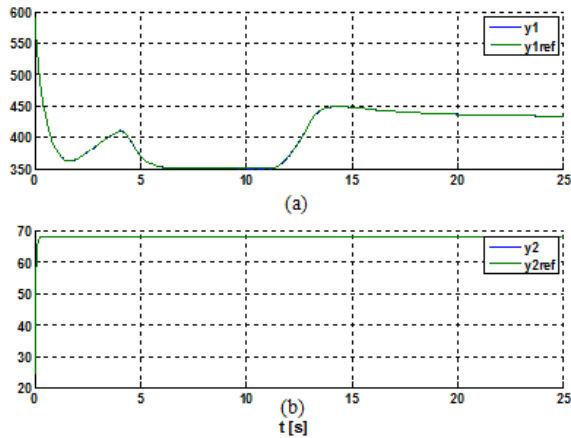


Fig. 11. Flat outputs of the system and their reference trajectories.

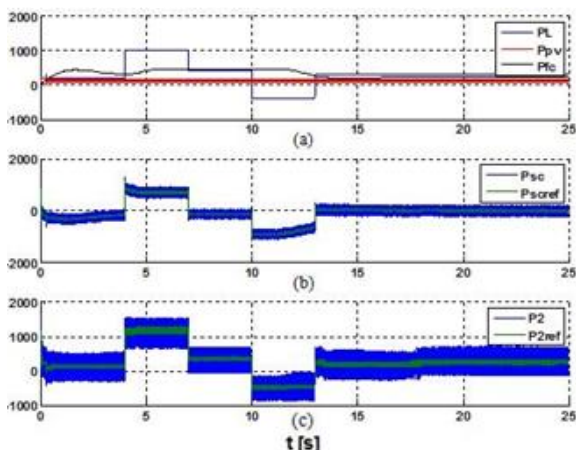


Fig. 12. Power waveforms of the system. (a) FC, SP and load power, (b) supercapacitor power and its reference waveform, (c) power of the DC-DC converter2 and its reference waveform.

To evaluate effect of the SP in the system, the voltage waveform of the system without SP is presented in the Fig.13. As it can be seen, although the HEPS is controlled well, the energy delivered to the SC in the normal operating mode ( $P_L < P_{FC}$ ) is

less than the previous system and so, the SC charges slower. Also, in the discharge operating mode ( $P_L > P_{FC}$ ), i.e.  $4s < t < 7s$ , SC delivers more energy to the load in comparison with the previous system. All the simulation results prove efficiency of the proposed control strategy in the studied system.

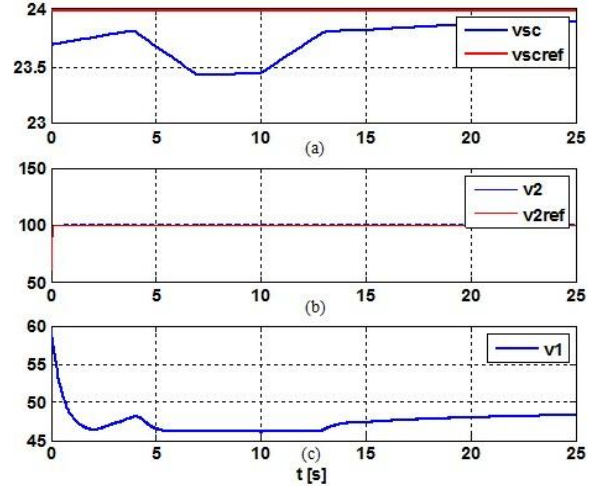


Fig. 13. Voltage waveforms of the system without SP,(a) voltages across the super capacitor bank and its reference, (b) output voltage and its reference, (c) variable DC bus voltage.

## 7. Conclusion

This paper presents an intelligent control strategy based on combination of the flatness based control technique and a MPPT based control method to manage the power flow in an electrical hybrid power source (EHPS). EHPS is composed of a fuel cell and a solar panel, as the main source and a super capacitor bank, as the auxiliary sources. For this purpose, the solar panel is such controlled that the maximum power can be extracted from it. The solar panel power is considered as a part of load power. Then, the other parts of the system is shown to be flat and so the energy is managed between fuel cell, SC and the new definition of the load, based on the flatness technique. It is carried out by planning the desired trajectories on the system output components to calculate the control variable of the system. The output components follow perfectly their own references which prove favourite operation of the EHPS to reply the high dynamic load power and to help the FC in overload mode. In this strategy, the power delivered by the FC is limited and its dynamics is controlled. The simulation results confirm the validity of the proposed control strategy in the studied topology. The output voltage stays always constant even when a high step load power is imposed to the system.

## References

- [1] K. Rajashekara, "Hybrid fuel-cell strategies for clean power generation," *IEEE Trans. Ind. Appl.*, vol. 41, no. 3, pp.682-688, 2005.
- [2] M. A. S. Masoum and M. Sarvi, "Voltage and current based MPPT of solar arrays under variable insolation and temperature conditions," in *Proc.of the 43rd International Universities Power Engineering Conference (UPEC '08)*, pp. 1-5, Padua, Italy, September 2008.
- [3] K. P. Adzakpa, K. Agbossou, Y. Dubé, M. Dostie, M. Fournier, and APoulin, "PEM fuel cells modeling and analysis through current and voltage transient behaviors," *IEEE Trans. Energy Convers.*, vol. 23, no.2, pp. 581-591, Jun. 2008.
- [4] P. Thounthong s. Rael and B. Davat, "Energy management of fuel cell/battery/supercapacitor hybrid power source for vehicle applications", Elsevier, *Journal of Power Sources*, pp. 376-385, 2009.
- [5] A. Rufer, "Power-Electronic interface for a supercapacitor-based energy storage substation in DC Transportation networks," *EPE'03*, Toulouse, October 2003.
- [6] M.Y. Ayad, S. Raël and B. Davat, "Hybrid power source using supercapacitors and batteries," *EPE'03*, Toulouse, October 2003.
- [7] S.M. Halpin, R.L. Spyker, R.M. Nelms and R.F. Burch, "Application of double-layer capacitor technology to static condensers for distribution system voltage control," *IEEE Trans.on Power Systems*, vol. 11, no. 4, Nov. 1996, pp. 1899-1904.
- [8] E. Schaltz, A. Khaligh and P. O. Rasmussen, "Investigation of Battery/Ultracapacitor Energy Storage Rating for a Fuel Cell Hybrid Electric Vehicle", in *Proc. 2008 IEEE Vehicle Power and Propulsion Conference (VPPC)*, Sep. 2008, China.
- [9] Z. Jiang, L. Gao, and R. A. Dougal, "Flexible multiobjective control of power converter in active hybrid fuel cell/battery power sources," *IEEE Trans. Power Electron.*, vol. 20, no. 1, pp. 244-253, Jan. 2005.
- [10] A. Payman, S. Pierfederici, F. Meibody-Tabar, "Energy Management in a Fuel Cell/Supercapacitor Multisource/Multiload Electrical Hybrid System," *IEEE Trans. Power Electron.*, vol. 24, no. 12, pp. 2681-2691, Dec. 2009.
- [11] A. Payman, et al., "An Adapted Control Strategy to Minimize DC-Bus Capacitors of a Parallel Fuel Cell/Ultracapacitor Hybrid System," *IEEE Trans. Power Electron.*, vol. 26, pp. 3843-3852, 2011.
- [12] A. Payman, S. Pierfederici, and F. Meibody-Tabar, "Energy control of supercapacitor/fuel cell hybrid power source," *J. Energy Conv. And Management*, vol. 49, Iss. 6, pp. 1637-1644, June 2008.
- [13] M.V. Nieuwstadt, M. Rathinam, and R.M. Murray, "Differential flatness and absolute equivalence," in *Proc. 1994, 33rd Conf. on Decision and Control*, vol. 1, pp. 326-332.
- [14] V. Kumaresh, et al., "Literature Review on Solar MPPT Systems," *Journal of Advance in Electronic and Electric Engineering.*, Vol. 4, no.3, pp.285-296, 2014.
- [15] M. Abdullah et al., "DSPACE Real-Time Implementation of MPPT- Based FLC Method," *International Journal of Photoenergy*, vol. 2013, Article ID 549273, 11 pages, 2013.